Relationship between temporal and spatial resolution for a constellation of GNSS-R satellites

Charles D. Bussy-Virat, Chris S. Ruf, Aaron J. Ridley

***Abstract*—Constellations of GNSS-R satellites improve the coverage of regions of interest by repeating measurements in a shorter period of time than with a single spacecraft. However, the temporal and spatial resolution of the samples are dependent on each other. Detecting short time scale changes is generally done with coarser spatial resolution. Likewise, detailed observations of a region with small scale features require longer intervals of time between observations. This study demonstrates the relationship between temporal and spatial resolution and its dependence on key mission design parameters such as the number of satellites, the number of orbit planes, and their inclination.**

***Index Terms*—Constellation, coverage, spatial resolution, temporal resolution, observations, GNSS-R, measurements.**

I. Introduction

With the recent advancements in small satellite technologies, the design of missions for the observation of the Earth has entered a new era. Low cost spacecraft now make practical the possibility of missions with multiple observatories in orbit, called constellations. A recent example is the Cyclone Global Navigation Satellite System (CYGNSS) [1]–[8]. Launched in December 2016, CYGNSS is a constellation of eight small satellites orbiting in a single plane at 520 km at an inclination of 35°. Its goal is to improve our understanding of rapid hurricane wind intensification by measuring surface wind speed from the strength of the specular reflection of GPS signals from the surface of the ocean. The measurement locations are referred to as specular points. There are typically about 10 GPS satellites visible at any time by a single CYGNSS satellite, resulting in about 10 potential specular points measurements to be made. Of these, the 4 with the highest receive antenna gains are sampled each second. The gain is a function of the incident angle of the specular point, with maximum gain occurring at 28° angle and lower gain toward either nadir or grazing incidence.

One of the key requirements of Earth observation missions is the coverage of regions of interest. Coverage can be quantified in terms of how quickly a certain percentage of an area is sampled by the measurement. Constellations allow measurements of the same region to be repeated in a shorter period of time than with a single spacecraft. The inclination of the orbits is a key parameter for the coverage. For example, the 35° inclination of the CYGNSS orbit plane optimizes the coverage at tropical latitudes, where most cyclones form and develop.

[9] evaluated the coverage performance of future GNSS-R Low Earth Orbit (LEO) constellations by simulating the sampling between a constellation of 8 LEO satellites and the four GNSS systems (GPS, Global Navigation Satellite System, Galileo and BeiDou Navigation Satellite System). In particular, they showed that the coverage was greatly improved compared to a configuration with only the GPS constellation, and that the spatial distribution of the specular point locations depended on the inclination of the LEO observatories' orbit. [10] showed that, under certain assumptions, GNSS-R satellite missions can be used to detect tsunamis and compared the global specular point distribution of two GNSS-R constellation configurations.

However, an important sampling issue arises in the case of GNSS-R measurements, which do not sample using contiguous swaths of samples as do most imagers. Instead, measurements are made along individual tracks as a specular point traverses the projected footprint of the receive antenna on the ground. The result, in the case of CYGNSS, is four tracks of individual samples per satellite that are typically between 500 and 1500 km long, depending on where the specular point enters and exits the antenna footprint. To determine the spatial coverage obtained over a particular interval of time, a region is segmented into a spatial grid and the number of cells sampled is determined over that interval of time. The percentage of cells sampled increases as the time interval increases but the rate at which it increases depends on the dimensions of the cells in the grid (spatial resolution). For example, it takes much longer to sample 90% of the cells in a grid if the cells are 1 km by 1 km than if they are 10 km by 10 km. This property essentially defines the relationship between spatial and temporal resolution. For a region where properties are changing quickly in time (e.g., the flood inundations during and after hurricanes), the short time scale changes are achievable with coarse spatial resolution but not with fine spatial resolution.

The goal of this study is to investigate the relationship between spatial and temporal resolution and to show its dependence on key mission design parameters, such as the number of satellites, the number of orbit planes, and their inclination. First, the approach followed and the metrics used to evaluate different properties of the coverage are detailed. Then, the relationship between temporal and spatial coverage is demonstrated and its dependence on key mission design parameters is analyzed, at low latitudes ($< 35°$) and high latitudes ($> 60°$) for constellations of satellites with different orbit inclination angles. Finally, the coverage performance of the CYGNSS constellation during the first year of the mission is presented.

Climate and Space Sciences and Engineering Department, University of Michigan, Ann Arbor, MI, 48109 USA e-mail: cbv@umich.edu

II. Methodology

A. Computing the locations of the specular points

To compute the position of a specular point, the locations of the CYGNSS and GPS observatories need to be determined. The Spacecraft Orbital Characterization Kit (SpOCK) [11] is an orbit propagator developed at the University of Michigan that predicts the trajectories of spacecraft in orbit with a high accuracy modeling of the dynamics. For example, LEO satellites (altitude $<$ 1,000 km, which is the altitude range the study focuses on), are subject to atmospheric drag, solar and Earth radiation pressure, gravitational perturbations due to the non-uniform mass distribution of the Earth and to gravity from the Sun and the Moon. These perturbing forces are modeled in SpOCK, allowing for an accurate computation of the trajectories.

Once the locations of the CYGNSS and the GPS are calculated, SpOCK determines the position of each specular point. It is defined as the location where a signal sent by a GPS reflects with equal angle of incidence and reflection on the surface of the Earth back to the target satellite (e.g., CYGNSS), as shown in Fig. 1. Because the receive power is quite important for the scientific measurement, a range-corrected gain is calculated. This is defined as: $\mathrm{RCG} = \frac{G}{R^2_{\mathrm{GPS}\to\mathrm{SP}} R^2_{\mathrm{SP}\to\mathrm{LEO}}}$, where G is the gain of the antenna, $R_{\mathrm{GPS}\to\mathrm{SP}}$ the distance from the GPS to the specular point, and $R_{\mathrm{SP}\to\mathrm{LEO}}$ the distance from the specular point to the LEO satellite. The locations of the specular points with the 4 highest range-corrected gains are considered. It is clear that missions that allow more than 4 simultaneous measurements and different antenna gain patterns will have different coverage statistics, but the general conclusions of this study should be applicable to any mission generally employing GNSS-R reflectometry techniques.

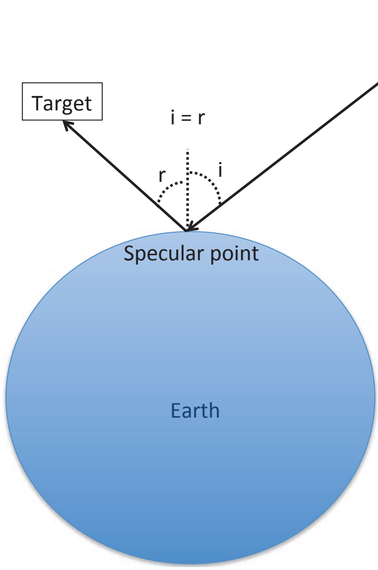

Fig. 1. Geometry of a specular point [11].

In order to study the relationship between temporal and spatial resolution, coverage statistics are needed. Metrics used in this study are the percentage coverage, the percentage revisited coverage, the time to reach a coverage goal of 90%, and the revisit times. The definition of these metrics and the methodology followed to compute them are now explained.

B. Definitions of metrics

The algorithm to compute the percentage coverage (also called simple coverage) was the following:

1) a rectangular region of the Earth was considered. A spatial grid covering the region was broken up into cells (of equal area);
2) the satellites were propagated in their orbits and specular points between the observatories and the GPS satellites were calculated every second;
3) the four specular points with the highest range-corrected gains for each LEO satellite were considered, while the rest were discarded;
4) for each specular point considered, the times of the measurements were noted in the appropriate spatial grid cells;
5) after all satellites were considered over a certain interval of time, the number of cells that had at least one time recorded were calculated;
6) this number was divided by the total number of cells in the grid and multiplied by 100% to provide the percentage coverage.

The percentage revisited coverage was defined in the same way except that a cell was counted if it had been visited at least twice.

At a given time, the coverage depends on the relative position of the grid with respect to the orbit plane, as there are gaps of time when the grid is not visible from the constellation due to the rotation of the Earth. However, the overall coverage after a given period of time does not depend on it, providing this time is longer than approximately one day. Therefore, for the analysis to be statistically meaningful, the coverage should be computed over a large number of relative positions of the orbit plane with respect to the grid. At a given latitude, the coverage was computed for different longitudinal placements of the grid and averaged over the different grids.

An example of the longitude-averaged coverage for a 500 km by 500 km grid at 20° latitude with a 10 km by 10 km resolution over 15 days for the CYGNSS constellation is shown in Fig. 2. The percentage coverage is represented as a solid blue line and the revisited coverage as a dashed blue line. The horizontal dashed red line depicts a coverage of 90%, which is defined as the coverage goal in this study. Although the revisited coverage increased relatively slowly for the first two days, both types of coverage converged to 100% before the end of the 15 day interval of time. The time to reach the coverage goal of 90% was $\sim$4.5 days, while $\sim$ 8 days were necessary to visit at least 90% of the cells twice.

The revisit times were calculated using the temporal data stored in the cells:

1) for every cell with at least two times stored in it, the time difference between all measurements within the cell was calculated;
2) all time differences of less than the time that it took for a satellite to cross a cell (a few seconds) were removed, as

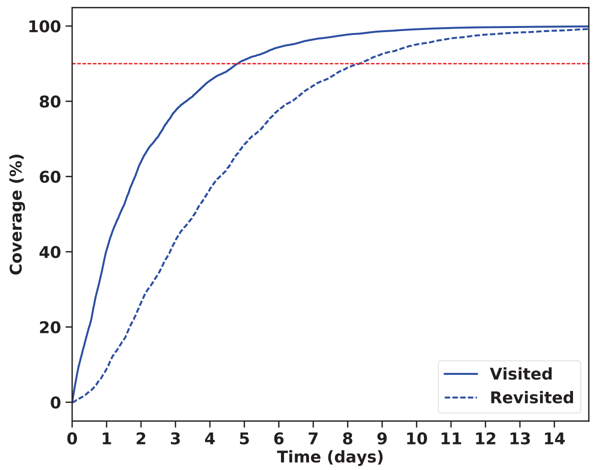

Fig. 2. Coverage and revisited coverage as a function of time. The grid was at 20° latitude and the cells were 10 km × 10 km.

these revisit times could correspond to the same satellite tracking the same specular point;

3) the average of the remaining time differences in all cells of the grid were computed.

There is a fundamental issue with this technique if it is applied over a short interval of time, such as one day. For a 24 hour simulation, the maximum allowable revisit time is 86399 seconds, which could only happen for the cells visited first and last in the day. For the cells encountered one second later, the maximum allowable revisit times is 86398 seconds. This trend continues through the day, so that a cell that is first encountered late in the day could only have, by definition, very short revisit times. This skews revisit times to very low values.

In order to overcome this problem, the interval of time needs to be large enough. Fig. 3 shows the mean revisit time (y-axis, also called repeat time) of the CYGNSS constellation for different durations of the simulations (x-axis): 25h, 50h, 69h, 75h, 83h, 104h, and 125h. The region considered here was the entire area between -35° and 35° latitude, and the dimensions of the cells were 25 km by 25 km. As the interval of time increased, longer revisit times could be included, which explains why the average revisit time increased. A fit (dashed line) converges to a value of 11.5 hours in ∼150 hours, implying that the true average revisit time is approximately 11.5 hours for this region. This figure shows that in order to calculate the true revisit time of the CYGNSS constellation measurements, at least 150 hours of data should be used.

C. Approach to study the relationship between temporal and spatial resolution

For the simulations considered here, the CYGNSS constellation was used as a baseline to study the coverage at latitudes below 35°. A region of 500 km by 500 km was considered and was placed at different latitudes to study the latitudinal dependence of the coverage: 5°, 10°, 15°, 20°, 25°, and 30°. As explained previously, the region was located at

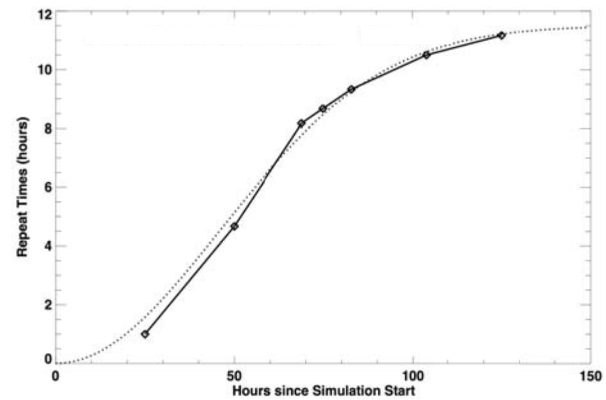

Fig. 3. Statistics (solid line) and fits to the revisit times (dotted line). The fit converges to 11.5 hours after ∼6 days.

different longitudes and the coverage was averaged over those longitudes. To study the relationship between temporal and spatial resolutions, the size of the cells of the grid mapping the 500 km by 500 km region was varied: 5 km × 5 km, 10 km × 10 km, 15 km × 15 km, 20 km × 20 km, and 25 km × 25 km. Fig. 4 shows examples of two different grid resolutions at two different latitudes. It illustrates the approach followed in the study: two parameters were varied, the latitude of the grid and the resolution of the cells in the grid. For each configuration, the percentage coverage, percentage revisited coverage, times to reach the 90% coverage goal, and revisit times were computed. The interval of time considered was 15 days, well above the minimum time necessary to accurately calculate revisit times (∼150 hours).

III. Results and Discussion

A. Relationship between temporal and spatial resolution

In Fig. 4, the percentage of cells visited was much larger for the bottom two grids, in which the cells were 25 km wide, than it was for the top two grids, in which the cells were 5 km wide, regardless of the latitude of the region. In other words, the percentage coverage, now simply referred to as coverage, depends on the spatial resolution of the grid. Furthermore, the satellite ground tracks bend at latitudes near the inclination of the orbit so that while the Earth has rotated between the overpasses of two consecutive satellites, the ground track of the next satellite still covers the region visited by the previous satellite. This is why the coverage increased faster at 30° (right two grids) than 5° latitude (left two grids).

Fig. 5 (top) shows the coverage for these four grids as a function of time over the 15 day simulation. The coverage increased more slowly for the smaller cells (red lines) than for the bigger cells (blue lines). The 90% coverage goal (horizontal black dashed line) was reached in ∼1 day at 30° latitude (blue solid line) and ∼2 days at 5° latitude (blue dashed line) for the larger celled grid. Approximately 9 days were necessary to cover 90% of the 5 km by 5 km cells at 30° latitude (red solid line) and more than 15 days were required at 5° latitude (red dashed line). Similar trends, but with about

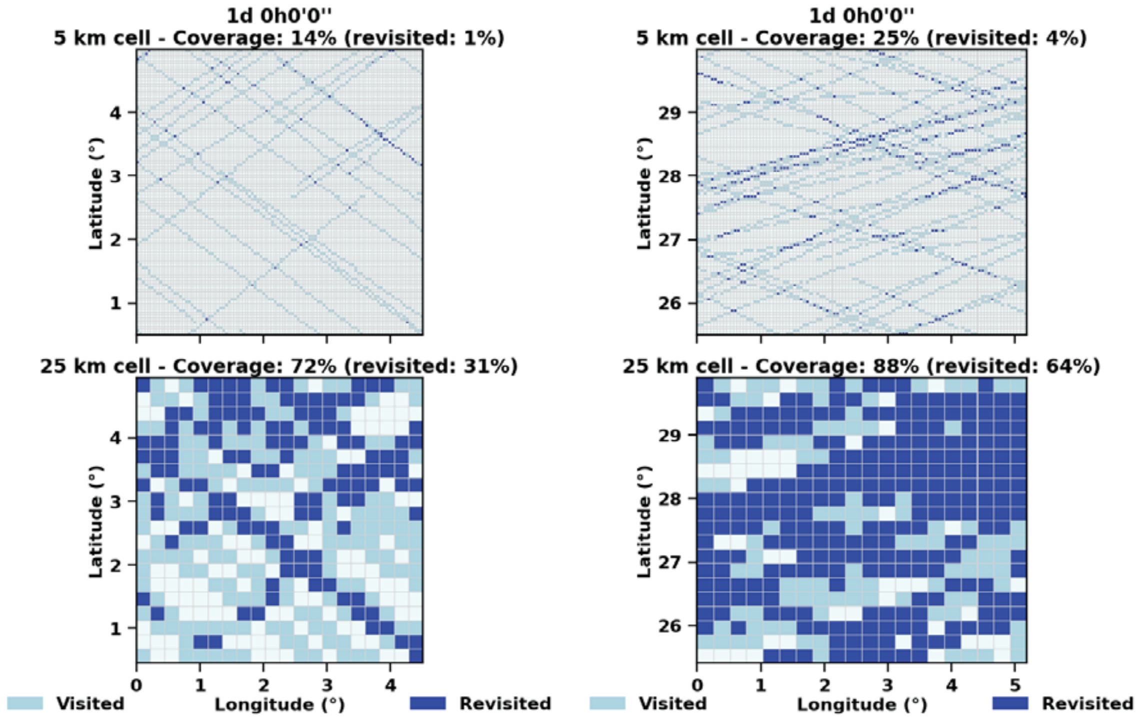

Fig. 4. Percentage coverage and revisited coverage after 24 hours of simulation. The cells in the top two grids were 5 km by 5 km and 25 km by 25 km in the bottom two grids. The left two grids mapped a region located at 5° latitude and the right two grids a region at 30° latitude. A cell was colored light blue if, after 24 hours, it had not been visited yet, blue if it had been visited exactly once, and dark blue if it had been visited at least twice.

double the time, were found for the revisited coverage, as shown in Fig. 5 (bottom).

The times to reach the 90% coverage goal for different latitudes of the grid (5° (black), 10° (blue), 15° (red), 20° (green), 25° (magenta) and 30° (yellow)) are reported in Fig. 6 (x-axis). The y-axis represents the different dimensions of the cells: 5 km $\times$ 5 km, 10 km $\times$ 10 km, 15 km $\times$ 15 km, 20 km $\times$ 20 km, and 25 km $\times$ 25 km. Both axes are in logarithm scale. Several observations can be made:

- as the latitude of the grid placement increased, it took less time to cover 90% of the cells, which is consistent with the observations made in Fig. 4;
- as the cells got smaller, the time to reach the coverage goal increased;
- this effect was more important at low latitudes than at higher latitudes, since the slopes are similar between each curve but the x-axis is in logarithm scale;
- the 90% coverage goal was not reached after 15 days of simulation if the region was at a lower latitude than 15° and the cells were 5 km by 5 km.

As described above, mean revisit times for each grid resolution were calculated by averaging the revisit times of all revisited cells in the grid and averaged over all longitudinal grids. Results are shown in Fig. 7. The x-axis corresponds to the latitude of the grid. For a given latitude of the grid, the average time between revisits was much larger for 5 km $\times$ 5 km cells than for larger cells. For instance, it took $\sim$82 hours to revisit a cell if it was 5 km by 5 km near the equator but less than 36 hours if it was 15 km by 15 km or larger. Moreover, regardless of the dimensions of the cells, the mean revisit time decreased as the latitude of the grid got closer to the inclination of the satellite constellation. At 30° latitude, the satellites were more likely to pass over the same cell since they were traveling almost longitudinally. This explains why the revisit times were smaller in average. Fig. 7 shows that this effect was stronger for smaller cells since the slope of the black curve is larger than the other curves.

B. Key mission design parameters

In this section, the effect of key mission design parameters on the relationship between spatial and temporal resolution is studied. More specifically, the times to reach the 90% coverage goal and the revisit times are compared between two configurations:

1) the CYGNSS constellation: 8 observatories in one plane at 35° inclination. This is the configuration studied in the previous section; and
2) the CYGNSS constellation + 8 satellites in a plane with inclinations of 35°, 65°, 75°, or 85° and local times of ascending node 6 hours from the CYGNSS constellation.

Fig. 8 shows an example of a configuration with the CYGNSS constellation and 8 satellites in a plane at 35°.

Fig. 9 shows the difference in time to reach the 90% coverage goal with the CYGNSS constellation minus the time to reach it with the combination of the CYGNSS constellation and the second plane at inclinations of 35°, 65°, 75°, or 85° (x-axis). The y-axis corresponds to the resolution of the cells. In other words, these plots show the time "saved" to reach the coverage goal by adding a second plane at different

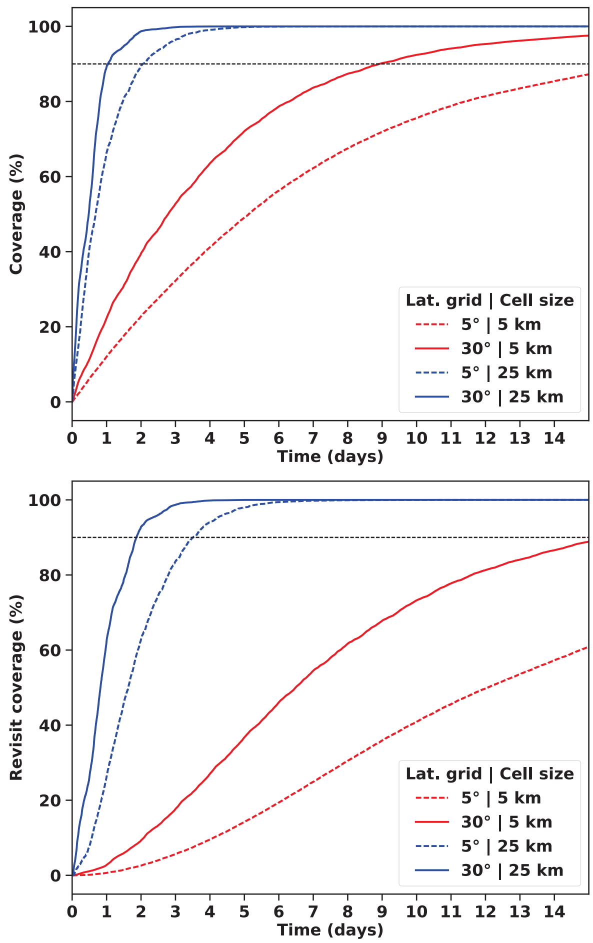

Fig. 5. Coverage as a function of time at 5° (dashed lines) and 30° latitude (solid lines). The cells were 5 km by 5 km (red lines) or 25 km by 25 km (blue lines). The top plot shows the percentage coverage and the bottom plot shows the percentage revisited coverage.

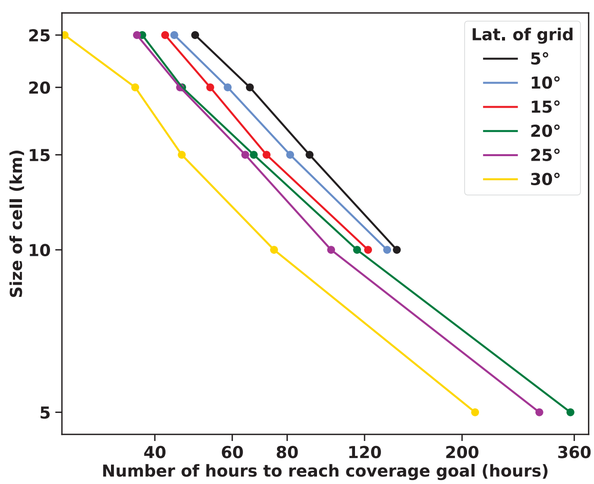

Fig. 6. Dimensions of the cells versus number of hours to reach the 90% coverage goal for different latitudes of the grid.

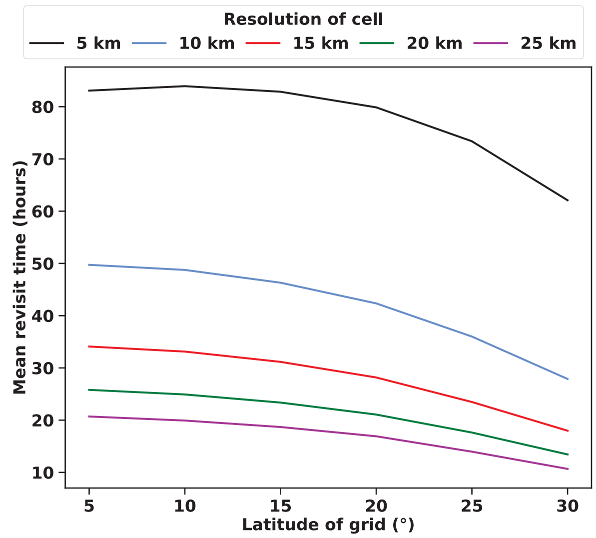

Fig. 7. Mean revisit times as a function of the latitude of the grid for different cell resolutions.

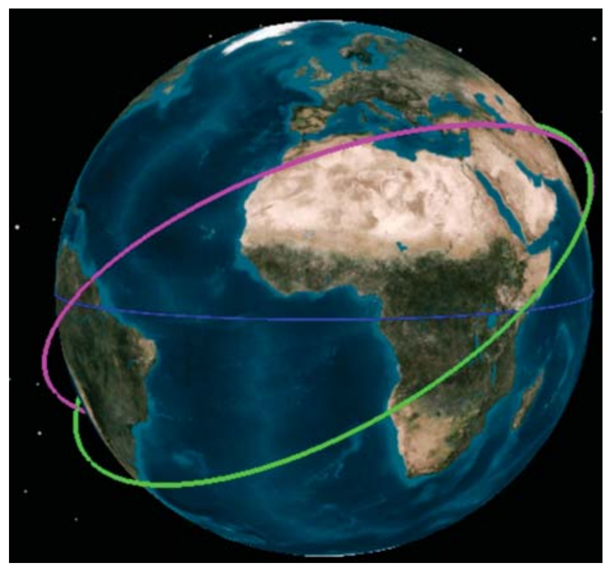

Fig. 8. Example of a configuration with the CYGNSS constellation (magenta) and 8 satellites in a plane at 35° (green). The coverage for different inclinations of the green plane are analyzed: 35°, 65°, 75°, and 85° (Satellite Tool Kit (STK) - Analytical Graphics, Inc (AGI))

inclinations, for different cell sizes. From Fig. 9, several observations can be made:

– adding a second plane significantly decreased the time to reach the coverage goal;
– this effect amplified rapidly as the cells got smaller (axes are in logarithm scale);
– the number of hours saved depended on the latitude of the grid. The maximum was obtained for a latitude of 20° (top right): more than 7 days were saved;
– the number of hours saved also depended on the inclination of the second plane. The constellation at 35° inclination improved the coverage much more than the constellations at 65°, 75° or 85° inclination, for which the improvements in coverage were similar;
– at a given latitude, the inclination of the plane mattered

more for small cells (similar slopes, in logarithm scale, between the configurations).

Fig. 10 shows the revisit times as a function of the latitude of the grid for the CYGNSS constellation and the combination of the CYGNSS constellation with the different planes. Two resolutions of the cells are shown: 5 km $\times$ 5 km (top) and 25 km $\times$ 25 km (bottom). The time to revisit a cell decreased with a second plane, particularly if it was at 35° inclination. The slope of the black line is larger than the slope of the other curves, which demonstrates that the improvement in the revisit time was better at low latitudes. Finally, by comparing the scale of the y-axis between both graphs, it can be concluded that adding a second plane reduced the average revisit time for smaller cells more effectively: 15-20 hours for 5 km $\times$ 5 km cells compared to 5-10 hours for 25 km $\times$ 25 km cells.

Fig. 9 and 10 demonstrate the effects of the orbit inclination on the coverage performance, particularly on the temporal resolution, as shown by the variations in the time to reach the 90% coverage goal and the revisit times. Overall, the regions at latitudes close to the inclination of the orbit planes were covered and revisited in a shorter amount of time. In addition, these effects increase with the spatial resolution. A second orbital parameter that may have an impact on the coverage is the number of orbit planes. To investigate these effects without changing the total number of satellites, the CYGNSS constellation was split in two orthogonal planes: 4 spacecraft in one plane and 4 spacecraft in a second plane with a difference of 6 hours in the local time of the ascending node.

In the case of the CYGNSS constellation, a cyclone is visited twice per day. Although the grid cells that are visited between the two passes vary, it is not necessary for exact revisits of the same cells to occur in order to get valuable information about the storm's evolution. To highlight this feature, larger cells were considered. A typical dimension of the R34 storm radius (the smallest radius outside of which the wind speeds are below 34 knots), 200 km, was chosen as the resolution of the grid. Fig. 11 shows the Probability Density Function (PDF) of the revisit times at 5° latitude for the two constellation configurations. The maximum revisit time during the 15 day simulation was 36 hours, meaning that all cells were visited at most every 36 hours. During the overpass of a constellation, flurries of samples were taken within a short interval of time, which explains the peak in the two distributions for revisit times smaller than about one orbit period. Since more satellites flew over the region during an overpass of the CYGNSS constellation, the peak was higher than with two orbit planes. The following pass occurred $\sim$12 hours later for the CYGNSS constellation, as shown by the portion of the blue distribution around 11-12 hours. With the two orbit plane configuration, the two planes flew over the region only every 6 hours, which explains the peak in the red distribution around $\sim$5-6 hours. Cells that were revisited only by one plane populated the portions of the PDF around $\sim$11, $\sim$23, and $\sim$35 hours. The peak around $\sim$17-18 hours corresponded to revisits during the second pass of the other orbit plane. Such results can be extrapolated to configurations with more than two orbit planes and with different separations between the local time of the ascending nodes.

Fig. 11 highlights a major advantage of constellations with multiple planes. The averages computed over revisit times larger than about an orbit period were 5.5 hours and 11 hours for the two orbit plane and one orbit plane configurations, respectively. Therefore, the important time separation between flurries of samples was decreased by a factor $\sim$2 with the two orbit plane configuration. However, placing satellites in different orbit planes can considerably increase the cost of the mission as it requires as many launches as the number of orbit planes.

C. Coverage at high latitudes

One of the major points of the previous section was that as the size of the cells decrease, the inclination of the plane matters more, both in terms of coverage and revisit times. In this section, this result is verified for the coverage of high latitudes ($> 60°$). The coverage and revisit time were computed for constellations of 8 spacecraft of different inclinations: 60°, 65°, 70°, 75°, 80°, 85°, and 90°.

Fig. 12 shows the percentage coverage (simple as solid lines, revisited as dashed lines) for different inclinations of the orbit plane, given a grid at 65° latitude. The cells in the grid were 5 km by 5 km (top) or 25 km by 25 km (bottom). For large cells (25 km wide, bottom plot), the inclination of the plane does not matter much. However, for small cells (5 km wide, top plot), the inclination is a key parameter. Indeed, the coverage obtained with the constellations at 65° and 70° inclination increase much faster than with the constellations at higher inclinations. The revisited coverage for the constellations at 65° and 70° inclination even exceeded the simple coverage for higher inclination constellations. In other words, after $\sim$12 days, the number of cells visited twice by the constellations at 65° and 70° is larger than the number of cells visited once by the constellations at 75°, 80°, 85°, and 90°.

If the grid is moved to a higher latitude, such as 80° as shown in Fig. 13, a similar observation is made: the inclination of the orbit matters more for small cells (5 km wide, top plot) than large cells (25 km wide, bottom plot). Interestingly, the constellation that optimizes the coverage for this latitude was the one at 85° inclination, followed by the constellation at 90° inclination. The differences were more important for the revisited coverage. The satellites in the orbit at 75° inclination had less specular point measurements within the grid so the coverage (simple and revisited) increased more slowly. Satellites with inclinations of 90° could measure specular points within a grid at 80° latitude almost every orbit, since near the pole, the satellites could see almost all of the GPS constellation.

D. Comparison of CYGNSS simulated results with actual mission coverage

CYGNSS mission requirement called for the coverage of the ocean surface between -35° and 35° latitude to be at least 70% over a 24-hour period of time to observe the evolution of cyclones during their lifetime. However, there were periods of time when the satellites could not take surface

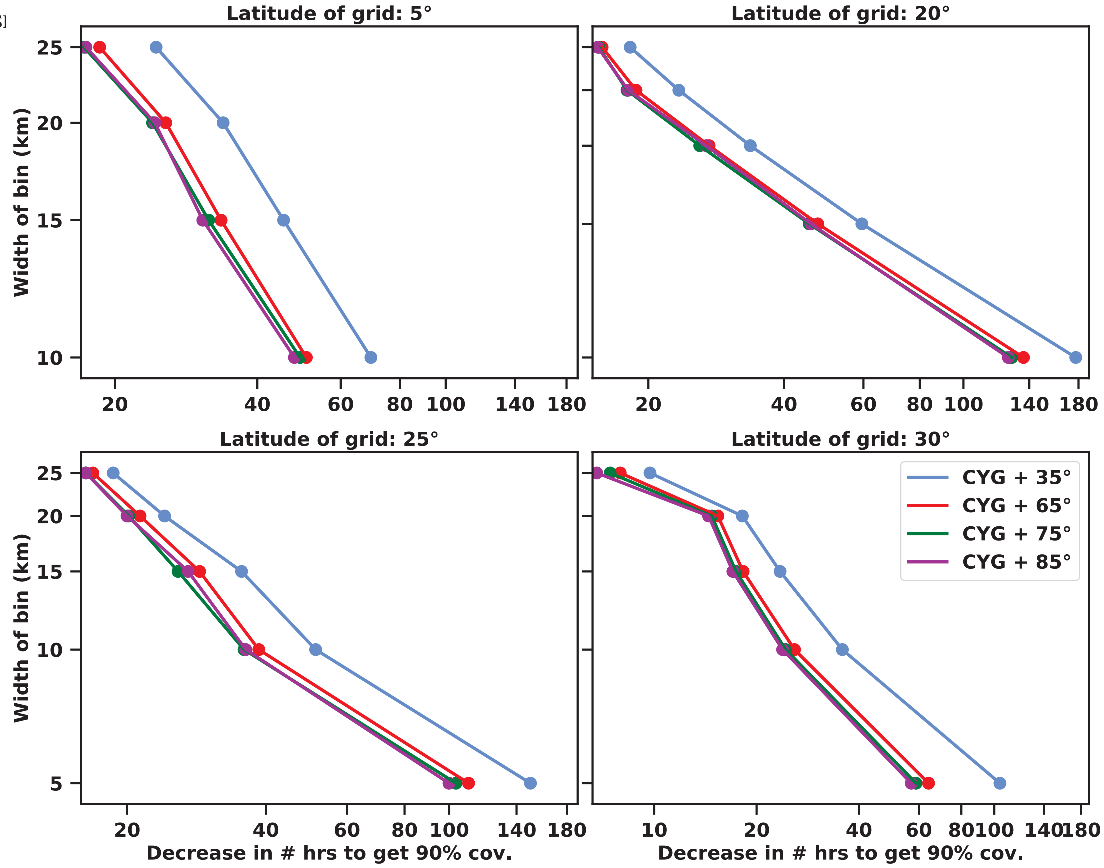

Fig. 9. Resolution of the cells as a function of the decrease in number of hours to reach the coverage goal from having a second plane at different inclinations. The grid in the top left plot is at 5° latitude, in the top right plot at 20° latitude, in the bottom left plot at 25° latitude, and in the bottom right plot at 30° latitude.

wind measurements, for different reasons. Until May 2017, the satellites were being commissioned so, at certain times, some of the satellites were not taking measurements. After May 2017, although the commissioning was almost over, differential drag maneuvers continued to be performed on the spacecraft to control their trajectories. During those times, the observatories were pitched by 82° so the antennas were not oriented toward the surface of the Earth. Furthermore, there were times when the orbit plane orientation with respect to the Sun was such that the satellites had to be rolled by ∼22° towards the Sun in order to meet the power requirements. Finally, when an anomaly occurred on a satellite, it was immediately switched to a safe mode and oriented directly towards the Sun. When any of these situations occurred, the satellite in question could not perform measurements, which considerably reduced the overall percentage coverage by the constellation. Fig. 14 shows the percentage coverage of the ocean surface between -35° and 35° latitude over 7 months of the mission (April to December 2017, top graph) and the number of satellites that were performing measurements at a given time (bottom graph). Overall, the coverage requirement of 70% was met ∼46% of the time. A correlation coefficient of 0.97 between the two graphs demonstrates the relationship between the percentage coverage and the number of satellites. When certain observatories were not performing measurements, the coverage dropped significantly. However, during the hurricane season (June - October), most of the satellites were operational so the coverage goal was reached ∼85% time. Fig. 14 puts in evidence the operational constraints that restrained the observations and limited the coverage of the oceans surface by the CYGNSS constellation. It also confirms the dependence of the coverage performance on the total number of observatories.

IV. Summary

A key requirement of Earth observation missions is the coverage of regions of interest. Constellations of GNSS-R satellites, such as CYGNSS, improve the spatial and temporal resolution of the coverage by allowing measurements to be repeated in a shorter period of time. However, detecting short time scale changes may necessitate to decrease the spatial resolution of the sampling. Reciprocally, covering a region with fine spatial resolution requires measurements to be made over a long period of time, but not with coarse spatial resolution. The study focused on the relationship between temporal and spatial resolution, as well as the effects of key mission design parameters on the coverage performance. Several results have been presented:

– the relationship between spatial resolution and temporal resolution has been investigated: the smaller the cells, the longer it takes to reach 90% coverage, and the longer the revisit time;
– this effect is stronger at equatorial latitudes than at latitudes near the inclination of the constellation, where the coverage maximizes and the revisit time minimizes; and

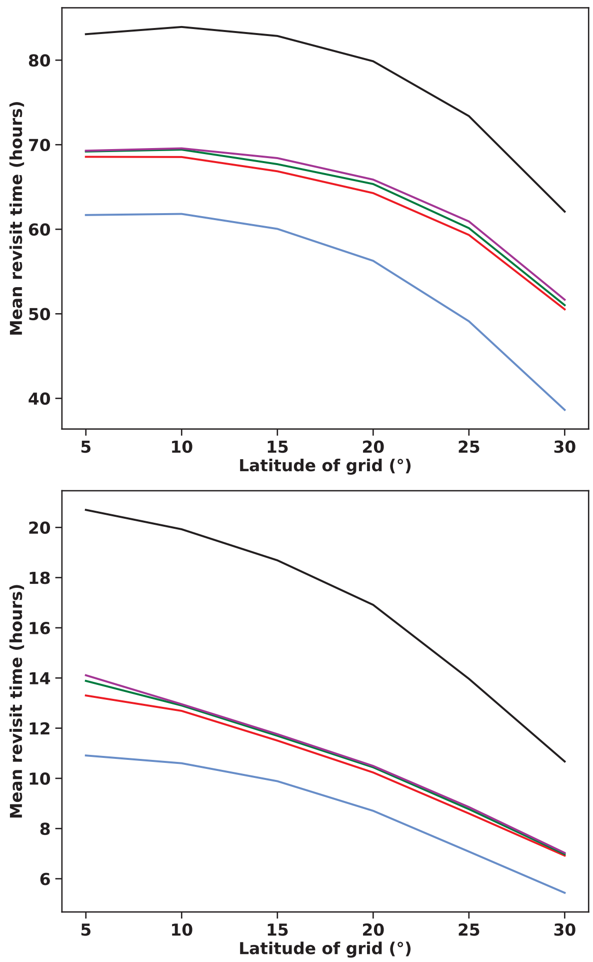

Fig. 10. Mean revisit time as a function of the latitude of the grid for different constellations: CYGNSS (black), CYGNSS + a second plane at 35° inclination (blue), 65° inclination (red), 75° inclination (green), or 85° inclination (magenta). The cells are 5 km by 5 km in the top graph and 25 km by 25 km in the bottom graph.

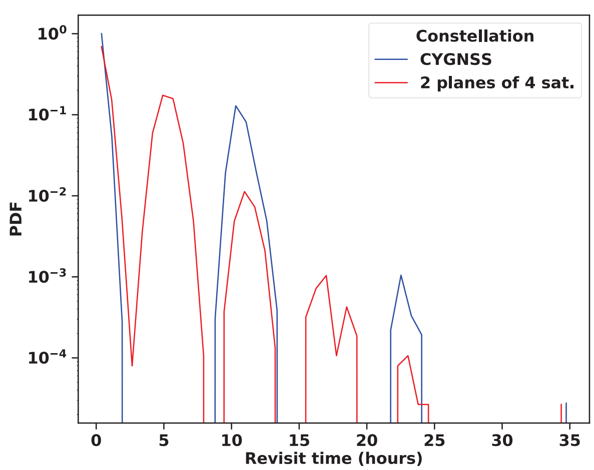

Fig. 11. Probability density distribution function of the revisit times for the one orbit plane configuration (labeled as CYGNSS, blue) and the two orbit plane configuration (red). The grid is at 5° latitude and the cells are 200 km by 200 km. The y-axis is in logarithm scale.

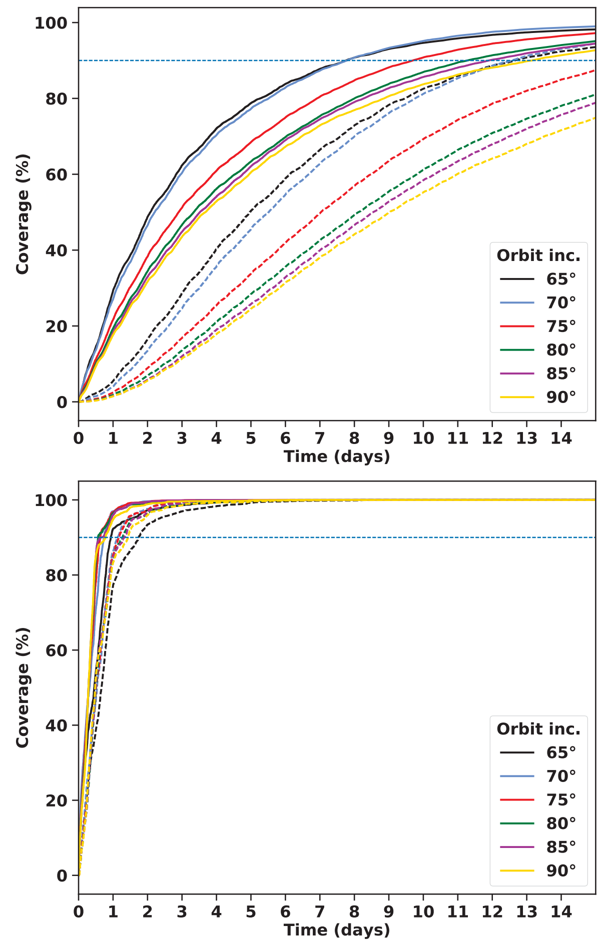

Fig. 12. Coverage as a function of time for different inclinations of the orbit planes. Solid lines represent the simple coverage and dashed lines the revisited coverage. The cells were 5 km by 5 km in the top plot and 25 km by 25 km in the bottom plot. The grids were at 65° latitude.

- as the size of the cells decreases, the inclination of the plane matters more, both in terms of coverage and revisit time.

Adding a second plane with 8 spacecraft significantly improves the coverage and revisit times:

- these improvements are more important for smaller cells than larger cells;
- the time required to reach a particular level of coverage is best reduced at 20-25° latitudes, while the revisit time is decreased mostly at low latitudes;
- the inclination of the plane is a key parameter in terms of coverage; and
- keeping the same total number of satellites but splitting the constellation in two planes decreases the time separation between two successive batches of samples.

Coverage analyses of regions at latitudes greater than 60° showed that similar results are verified for the coverage performance at high latitudes. For mission design, the key parameters that have the largest effects on the coverage performance are the number of satellites, the number of orbit planes, their relative orientation, and their inclination. These effects are

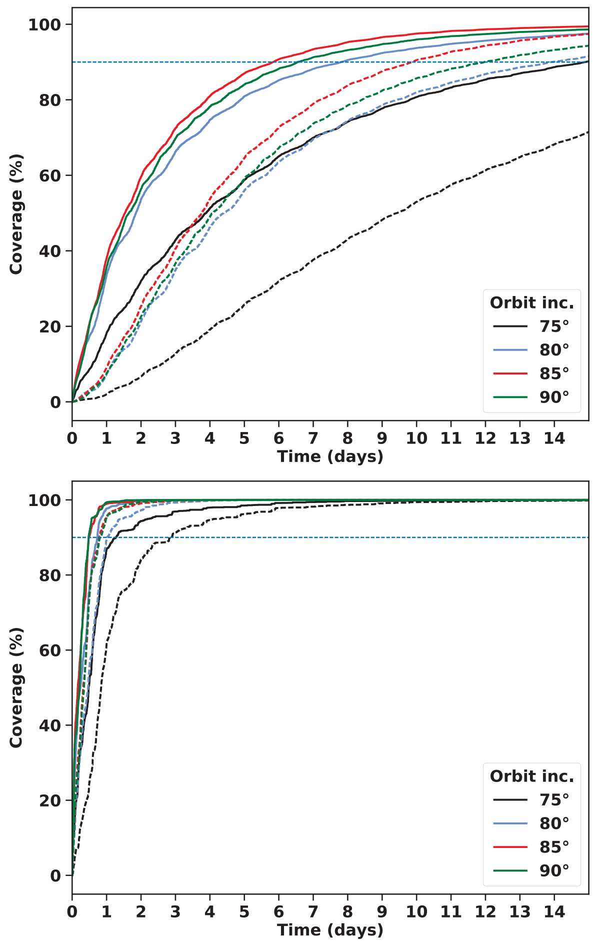

Fig. 13. Coverage as a function of time for different inclinations of the orbit planes. Solid lines represent the simple coverage and dashed lines the revisited coverage. The cells were 5 km by 5 km in the top plot and 25 km by 25 km in the bottom plot. The grids were at 80° latitude.

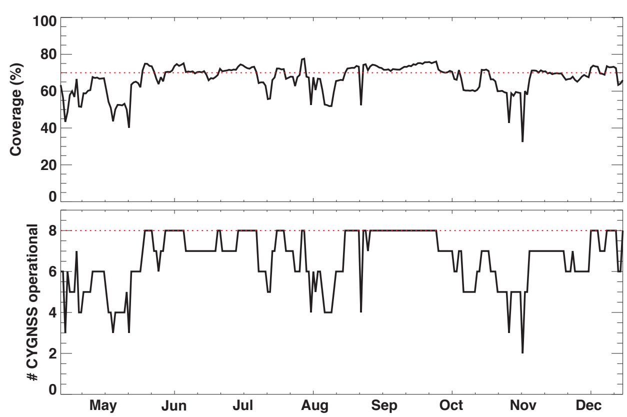

Fig. 14. Top: Actual percentage coverage over the ocean surface between -35° and 35° latitude over 7 months by the CYGNSS constellation. The coverage requirement of 70% is indicated as a red dotted line; bottom: number of CYGNSS satellites taking measurements at a given time. The total number of CYGNSS satellites (8) is indicated as a red dotted line.

particularly important for high spatial resolution coverage.

Finally, the actual percentage coverage of the oceans surface by the CYGNSS constellation over 7 months was presented. Operational constraints prevented some of the satellites from performing measurements at certain times of the mission, during which the overall coverage by the constellation decreased. This analysis validated the dependence of the coverage performance on the number of satellites, and showed how operations limited the observations.

Acknowledgment

This research was funded in part by NASA Science Mission Directorate Contract NNL13AQ00C.

References

[1] C. S. Ruf, S. Gleason, Z. Jelenak, S. Katzberg, A. Ridley, R. Rose, J. Scherrer, and V. Zavorotny, "The cygnss nanosatellite constellation hurricane mission," in *Geoscience and Remote Sensing Symposium (IGARSS), 2012 IEEE International*. IEEE, 2012, pp. 214–216.

[2] D. Rose, M. Vincent, R. Rose, and C. Ruf, "The cygnss ground segment; innovative mission operations concepts to support a micro-satellite constellation," in *Aerospace Conference, 2013 IEEE*. IEEE, 2013, pp. 1–9.

[3] C. Ruf, M. Unwin, J. Dickinson, R. Rose, D. Rose, M. Vincent, and A. Lyons, "Cygnss: enabling the future of hurricane prediction [remote sensing satellites]," *IEEE Geoscience and Remote Sensing Magazine*, vol. 1, no. 2, pp. 52–67, 2013.

[4] C. Ruf, A. Lyons, and A. Ward, "Nasa intensifies hurricane studies with cygnss," *Earth Observer, NASA*, vol. 25, no. 3, pp. 12–21, 2013.

[5] C. Ruf, P. Chang, M. Clarizia, S. Gleason, Z. Jelenak, J. Murray, M. Morris, S. Musko, D. Posselt, D. Provost, D. Starkenburg, and V. Zavorotny, *CYGNSS Handbook*. Michigan Pub, 2016.

[6] C. S. Ruf, R. Atlas, P. S. Chang, M. P. Clarizia, J. L. Garrison, S. Gleason, S. J. Katzberg, Z. Jelenak, J. T. Johnson, S. J. Majumdar *et al.*, "New ocean winds satellite mission to probe hurricanes and tropical convection," *Bulletin of the American Meteorological Society*, vol. 97, no. 3, pp. 385–395, 2016.

[7] J. Murray, C. Ruf, N. Baker, T. Lang, E. Uhlhorn, D. Masters, G. Halliwell, K. Carey, D. Helms, V. Escobar *et al.*, "Report on the nasa cygnss mission applications workshop," 2016.

[8] J. A. Crespo, D. J. Posselt, C. M. Naud, and C. Bussy-Virat, "Assessing cygnsss potential to observe extratropical fronts and cyclones," *Journal of Applied Meteorology and Climatology*, vol. 56, no. 7, pp. 2027–2034, 2017.

[9] F. Gao, T. Xu, N. Wang, C. Jiang, Y. Du, W. Nie, and G. Xu, "Spatiotemporal evaluation of gnss-r based on future fully operational global multi-gnss and eight-leo constellations," *Remote Sensing*, vol. 10, no. 1, p. 67, 2018.

[10] R. Stosius, G. Beyerle, A. Helm, A. Hoechner, and J. Wickert, "Simulation of space-borne tsunami detection using gnss-reflectometry applied to tsunamis in the indian ocean," *Natural Hazards and Earth System Sciences*, vol. 10, no. 6, p. 1359, 2010.

[11] C. Bussy-Virat, J. Getchius, and A. Ridley, "The spacecraft orbital characterization kit and its applications to the cygnss mission." in *2018 Space Flight Mechanics Meeting*, 2018, p. 1973.

Charles D. Bussy-Virat graduated with a MEng in aerospace engineering at the Institut Superieur de l'Aeronautique et de l'Espace - SUPAERO in Toulouse, France. He received a Ph.D. in spaceflight dynamics at the University of Michigan during which he conducted research on spacecraft collision avoidance and space mission design. As a Research Fellow at the University of Michigan, he is currently involved in the NASA Cyclone Global Navigation Satellite System mission and works on orbit determination, spacecraft orbit modeling, and space weather effects on satellite trajectories.

Chris S. Ruf (S85 M87 SM92 F01) received the B.A. degree in physics from Reed College, Portland, OR, and the Ph.D. degree in electrical and computer engineering from the University of Massachusetts at Amherst. He is currently Professor of atmospheric science and space engineering at the University of Michigan; and Principal Investigator of the NASA Cyclone Global Navigation Satellite System mission. He has worked previously at Intel Corporation, Hughes Space and Communication, the NASA Jet Propulsion Laboratory, and Penn State University. His research interests include GNSS-R remote sensing, microwave radiometry, atmosphere and ocean geophysical retrieval algorithm development, and sensor technology development. Dr. Ruf is a member of the American Geophysical Union (AGU), the American Meteorological Society (AMS), and Commission F of the Union Radio Scientifique Internationale. He is former Editor-in- Chief of the IEEE Transactions on Geoscience and Remote Sensing and has served on the editorial boards of Radio Science and the Journal of Atmospheric and Oceanic Technology. He has been the recipient of four NASA Certificates of Recognition and seven NASA Group Achievement Awards, as well as the 1997 TGRS Best Paper Award, the 1999 IEEE Resnik Technical Field Award, the 2006 IGARSS Best Paper Award, and the 2014 IEEE GRSS Outstanding Service Award.

Aaron J. Ridley received a B.S. in physics from Eastern Michigan University, Ypsilanti, MI, and a Ph.D. degree in Atmospheric and Space Sciences from the University of Michigan. He is currently a Professor of Space Sciences at the University of Michigan; and Constellation Scientist of the NASA Cyclone Global Navigation Satellite System mission. He has worked at the National Center for Atmospheric Research, and Southwest Research Institute. His interests include modeling the dynamics and electrodynamics of the near-Earth space environment. In addition, he has been the Principal Investigator of four CubeSats, two of which are in currently in orbit. Prof. Ridley is a member of the American Geophysical Union (AGU), was Secretary for the AGU Space Physics and Aeronomy, Magnetospheric Physics section and served on science steering committees for the National Science Foundation and several committees for the National Academy of Sciences. He has the most cited paper from 2005-2010 from the Journal of Atmospheric and Solar Terrestrial Research, and won a variety of research and teaching awards from the University of Michigan.